

Effect of dislocations on electrical and optical properties of *n*-type $\text{Al}_{0.34}\text{Ga}_{0.66}\text{N}$

K. X. Chen,¹ Q. Dai,¹ W. Lee,² J. K. Kim,³ E. F. Schubert,^{1,3,a)} J. Grandusky,⁴ M. Mendrick,⁴ X. Li,⁴ and J. A. Smart⁴

¹*Department of Physics, Applied Physics, and Astronomy, Future Chips Constellation, Rensselaer Polytechnic Institute, Troy, New York 12180, USA*

²*Future Chips Constellation, Engineering Science Program, Rensselaer Polytechnic Institute, Troy, New York 12180, USA*

³*Department of Electrical, Computer, and Systems Engineering, Future Chips Constellation, Rensselaer Polytechnic Institute, Troy, New York 12180, USA*

⁴*Crystal IS, Inc., 70 Cohoes Avenue, Green Island, New York 12183, USA*

(Received 8 September 2008; accepted 20 October 2008; published online 11 November 2008)

The effect of edge and screw dislocations on the electrical and optical properties of *n*-type $\text{Al}_{0.34}\text{Ga}_{0.66}\text{N}$ is investigated. It is found that edge dislocations strongly affect the electrical properties of *n*-type $\text{Al}_{0.34}\text{Ga}_{0.66}\text{N}$. Both free carrier concentration and mobility decrease with increasing edge dislocation density. Edge dislocations also enhance nonradiative recombination, which is indicated by decreasing near-band-edge UV as well as parasitic blue photoluminescence. The UV/blue ratio is found to be independent of the edge dislocation density but strongly depends on the Si doping concentration. © 2008 American Institute of Physics. [DOI: 10.1063/1.3021076]

GaN-based semiconductor and its aluminum- and indium-containing alloys have numerous applications in optoelectronic and microelectronic devices, such as light-emitting diodes (LEDs) and laser diodes, and high electron mobility transistors. Most of the GaN-based materials and devices are grown on sapphire or SiC substrates due to the lack of high quality native bulk substrates. The large lattice and thermal mismatch between III-nitrides and sapphire substrates results in a high density of threading dislocations ranging between 10^7 and 10^{11} cm^{-2} .¹ Transmission electron microscopy investigations have shown high screw dislocation densities near the substrate-buffer interface, as well as high edge dislocation densities threading from the substrate-buffer interface to the epilayer surface.¹ These threading dislocations may introduce energy levels within the band gap of GaN or AlGaIn, which adds an additional recombination path other than the near-band-edge recombination.²⁻⁷ Threading dislocations may also act as scattering centers and thus affect carrier transport.^{1,2,8-10} In this letter, the effect of edge and screw dislocations on the electrical and optical properties of *n*-type $\text{Al}_{0.34}\text{Ga}_{0.66}\text{N}$ is investigated.

Samples are grown by metal-organic vapor-phase epitaxy (MOVPE). Trimethylgallium (TMGa), trimethylaluminum (TMAI), and ammonia (NH_3) are used as precursors for Ga, Al, and N, respectively. Diluted silane (SiH_4) is used as the *n*-type dopant source. First, eight AlN templates with different dislocation densities are grown on *c*-plane sapphire substrates. Among these eight AlN templates, six of them are grown using a two-step growth technique, which involves a low-temperature AlN (825 °C) nucleation layer with different thicknesses and growth conditions, followed by a 300-nm-thick high-temperature (HT) AlN layer (1200 °C). The other two AlN templates are grown using a flow-modulation (FM) technique, during which TMAI and NH_3 are introduced into the reactor chamber in a pulse sequence

at a high growth temperature (1200 °C). After the repetition of pulse sequences, TMAI and NH_3 are changed to a continuous-flow mode to grow a 300-nm-thick HT AlN layer. The surface morphology and crystalline quality of AlN templates are characterized by atomic force microscope (AFM) and x-ray diffraction (XRD). It is found that the AlN templates grown using the FM technique have smaller full width at half maximum (FWHM) for XRD (002) and (102) rocking curves, indicating a better crystalline quality compared to the two-step-growth AlN template. After the AFM and XRD characterizations, the eight AlN templates with different dislocation densities are reloaded into the MOVPE system for regrowth. Ten periods of $\text{Al}_{0.5}\text{Ga}_{0.5}\text{N}/\text{AlN}$ superlattice and a 1- μm -thick *n*-type AlGaIn are grown on top of the AlN templates. Two series of samples with different SiH_4 flow rates, which are 7.88×10^{-9} and 7.88×10^{-10} mol/min, respectively, are grown. After the growth, van der Pauw pattern Hall effect measurement measured the electron mobility and concentration. A frequency-quadrupled Nd doped yttrium aluminum garnet laser with emission wavelength of 266 nm is used as the excitation source for photoluminescence (PL) measurements.

The electron mobility and concentration versus edge dislocation densities of *n*-type $\text{Al}_{0.34}\text{Ga}_{0.66}\text{N}$ are shown in Fig. 1. It has been reported that the FWHMs of XRD (002) and (102) rocking curves indirectly represent the screw and edge dislocation densities.^{11,12} We calculate the screw and edge dislocation densities by using the formula provided in Ref. 12, which reveals the relation between the XRD rocking curve and the dislocation density. Vegard's law is used for the calculation of the lattice parameters of *n*-type $\text{Al}_{0.34}\text{Ga}_{0.66}\text{N}$. Figure 1 shows that the electron mobility decreases from 80 to 10 $\text{cm}^2/\text{V s}$ as the edge dislocation density increases. It was reported that an acceptorlike trap level is formed due to the dangling bonds along the edge dislocation lines.¹ In *n*-type GaN or AlGaIn, this acceptorlike trap will be filled and therefore carries one electron charge. The negatively charged dislocation lines act as Coulomb scatter-

^{a)}Electronic mail: efschubert@rpi.edu.

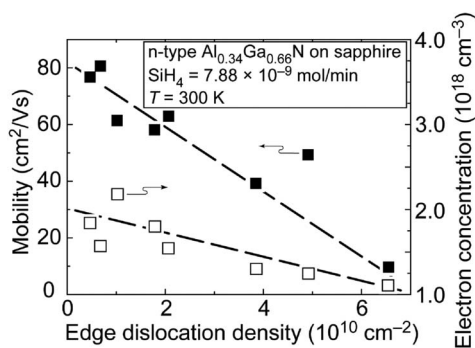


FIG. 1. Electron mobility (solid square) and concentration (open square) vs the edge dislocation density of *n*-type $\text{Al}_{0.34}\text{Ga}_{0.66}\text{N}$. The dash lines are guide to the eye.

ing centers and reduce the electron mobility. Figure 1 also shows that the electron concentration decreases by a factor of 2 as the edge dislocation density increases from 4.7×10^9 to $6.6 \times 10^{10} \text{ cm}^{-2}$, even though a fixed SiH_4 flow rate of $7.88 \times 10^{-9} \text{ mol/min}$ is maintained during the growth of this set of samples. The acceptorlike traps formed by the dangling bonds along the edge dislocation lines may compensate the Si dopant and thus reduce the free electron concentration.⁹ In contrast to the strong dependence on the edge dislocations, the electron mobility and concentration show a weaker dependence on the dislocations with a screw component (not shown here). Allerman *et al.*¹³ also reported a similar phenomenon where the sheet resistance of Si-doped AlGaIn had a stronger dependence on edge dislocations than on screw dislocations. The stronger effect of edge dislocations on the electrical properties of *n*-type AlGaIn can be explained by the fact that the density of dislocations with an edge component is usually one order of magnitude higher than the density of dislocations with a screw component,¹³ resulting in a stronger interaction between electrons and edge dislocations.

Figure 2 shows the room-temperature PL spectrum of two *n*-type AlGaIn samples with different Al compositions. Both of them show a sharp near-band-edge emission at a shorter wavelength, which we will denote as the “UV emission.” Besides the UV emission, there is another broad luminescence band at a longer wavelength, which we will refer to as the “parasitic emission.” The parasitic emission in Si-doped AlGaIn was found to originate from the acceptorlike compensating native defects. It has a similar nature as the yellow luminescence in GaN.¹⁴ The peak wavelength of

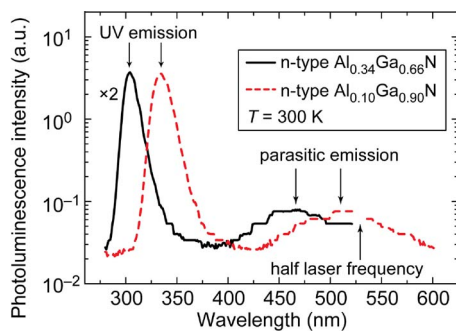


FIG. 2. (Color online) PL spectrum of *n*-type $\text{Al}_{0.34}\text{Ga}_{0.66}\text{N}$ (black line) and $\text{Al}_{0.10}\text{Ga}_{0.90}\text{N}$ (red dashed line). The spectrum is cut off at 532 nm, which is the half frequency of the 266 nm laser.

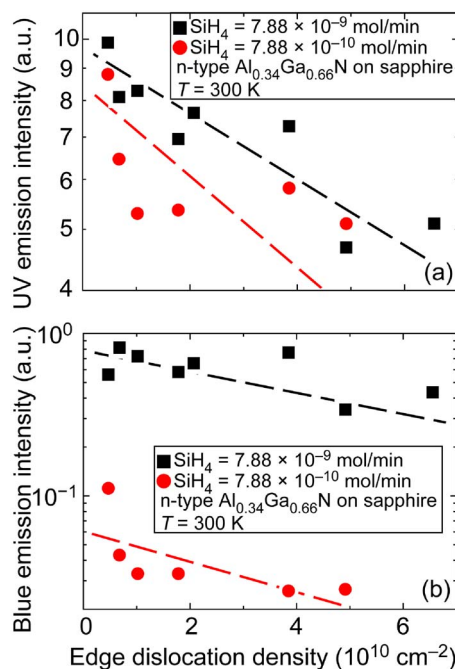


FIG. 3. (Color online) PL intensity of (a) UV and (b) parasitic blue emissions vs the edge dislocation density of *n*-type $\text{Al}_{0.34}\text{Ga}_{0.66}\text{N}$. Two series of samples with different SiH_4 flow rates, which are 7.88×10^{-9} (black square) and $7.88 \times 10^{-10} \text{ mol/min}$ (red circle), respectively, are shown. The dash lines are guide to the eye.

the UV emission blueshifts from 334 nm (3.72 eV) for $\text{Al}_{0.10}\text{Ga}_{0.90}\text{N}$ to 304 nm (4.09 eV) for $\text{Al}_{0.34}\text{Ga}_{0.66}\text{N}$. Meanwhile, the peak wavelength of the parasitic emission also shifts from 510 nm (2.44 eV) down to 460 nm (2.70 eV). It is worth noting that the change of the UV emission energy ($\Delta E_1 = 0.37 \text{ eV}$) is larger than the change in the parasitic emission energy ($\Delta E_2 = 0.26 \text{ eV}$). This difference indicates that the acceptorlike defect energy level which causes the parasitic emission becomes deeper in AlGaIn as the Al composition increases.

The PL intensity of UV and parasitic blue emission versus the edge dislocation densities of *n*-type $\text{Al}_{0.34}\text{Ga}_{0.66}\text{N}$ is shown in Figs. 3(a) and 3(b), respectively. It is found that both UV and parasitic blue emission intensities decrease with increasing edge dislocation densities. The decreasing trend of PL intensities of both UV and parasitic blue emission implies that the nonradiative recombination is stronger at higher edge dislocation densities. However, similar decreasing trend is not observed when plotting the UV and parasitic blue emission intensities versus the screw dislocation density. Instead, randomly scattering data points are observed. The effect of different types of dislocations on the optical properties of nitride material is still controversial. Some reports showed that screw dislocations act as nonradiative recombination centers,^{3,15} while the others concluded that edge dislocations act as nonradiative recombination centers.^{16,17} Figure 3 indicates that edge dislocations have a strong effect on the optical properties of *n*-type AlGaIn. Figure 3 also shows that the UV emissions from two sets of samples with different SiH_4 flow rates have similar intensities. On the contrary, the parasitic blue emission intensities decrease by one order of magnitude when SiH_4 flow rate is decreased from 7.88×10^{-9} to $7.88 \times 10^{-10} \text{ mol/min}$. The parasitic blue emission intensity is proportional to the Si doping concentration. A

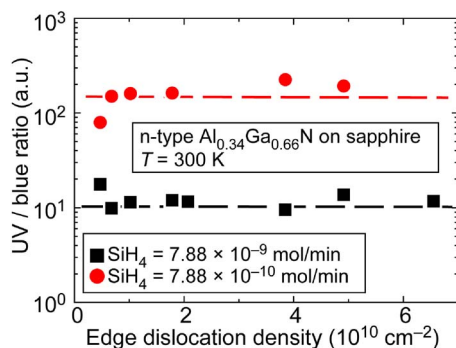


FIG. 4. (Color online) PL intensity ratio between UV and parasitic blue emissions vs the edge dislocation density of *n*-type $\text{Al}_{0.34}\text{Ga}_{0.66}\text{N}$. The dashed lines are guide to the eye.

similar proportional behavior has also been reported for the yellow luminescence in GaN.^{7,18} This relation indicates that the parasitic blue emission originates from acceptorlike compensating native defects because the defect concentration is proportional to the doping concentration.¹⁴

The intensity ratio between the UV and parasitic blue emission is shown in Fig. 4. Since the parasitic blue emission intensity is proportional to the doping concentration but the UV emission intensity is not affected by the Si doping, the UV/blue ratio increases by one order of magnitude when SiH_4 flow rate decreases from 7.88×10^{-9} to 7.88×10^{-10} mol/min. Furthermore, Fig. 4 shows that the UV/blue ratio does not have a clear dependence on the edge dislocation density. Elsner *et al.*⁵ suggested that the threading dislocations were likely to trap group-III vacancies or vacancy-oxygen complexes, which increase the intensity of parasitic emission. However, our result implies that the amount of defects trapped by threading dislocations may be much less than the total amount of compensating native defects introduced by Si doping. Therefore, the intensity of the parasitic emission in Si-doped AlGaN is mainly determined by the native defect density, which in turn is proportional to the Si doping concentration.¹⁴ It is worth pointing out that the threading dislocations still play an important role in determining the recombination mechanism of AlGaN-based UV LEDs under different injection currents. The UV/blue ratio shows different dependences on the injection current with different threading dislocation densities.¹⁹

In conclusion, the effect of edge and screw dislocations on the electrical and optical properties of *n*-type $\text{Al}_{0.34}\text{Ga}_{0.66}\text{N}$ is investigated. Both free carrier concentration and mobility decrease with increasing edge dislocation densities. The acceptorlike traps formed by the dangling bonds

along the edge dislocation lines act as Coulomb scattering centers and also compensate the Si dopant. The energy level of these compensating native defects becomes deeper in AlGaN as the Al composition increases. The edge dislocations also act as nonradiative recombination centers, which are implied by a decreasing PL intensity versus edge dislocation density. The UV/blue ratio is found to be independent of the edge dislocation density, but it strongly depends on the Si doping concentration.

Support from Crystal IS, DOE, NSF, Samsung Electro Mechanics Co., Sandia National Laboratories, and New York State is gratefully acknowledged. The authors would like to acknowledge Dr. Leo J. Schowalter from Crystal IS for useful discussions.

- ¹N. G. Weimann, L. F. Eastman, D. Doppalapudi, H. M. Ng, and T. D. Moustakas, *J. Appl. Phys.* **83**, 3656 (1998).
- ²D.-S. Jiang, D.-G. Zhao, and H. Yang, *Phys. Status Solidi B* **244**, 2878 (2007).
- ³T. Hino, S. Tomiya, T. Miyajima, K. Yanashima, S. Hashimoto, and M. Ikeda, *Appl. Phys. Lett.* **76**, 3421 (2000).
- ⁴S. J. Rosner, E. C. Carr, M. J. Ludowise, G. Girolami, and H. I. Erikson, *Appl. Phys. Lett.* **70**, 420 (1997).
- ⁵J. Elsner, R. Jones, M. I. Heggie, P. K. Sitch, M. Haugk, Th. Frauenheim, S. Oberg, and P. R. Briddon, *Phys. Rev. B* **58**, 12571 (1998).
- ⁶S. Yu. Karpov and Y. N. Makarov, *Appl. Phys. Lett.* **81**, 4721 (2002).
- ⁷D. G. Zhao, D. S. Jiang, H. Yang, J. J. Zhu, Z. S. Liu, S. M. Zhang, J. W. Liang, X. Li, X. Y. Li, and H. M. Gong, *Appl. Phys. Lett.* **88**, 241917 (2006).
- ⁸D. C. Look and J. R. Sizelove, *Phys. Rev. Lett.* **82**, 1237 (1999).
- ⁹D. G. Zhao, H. Yang, J. J. Zhu, D. S. Jiang, Z. S. Liu, S. M. Zhang, Y. T. Wang, and J. W. Liang, *Appl. Phys. Lett.* **89**, 112106 (2006).
- ¹⁰Y. Taniyasu, M. Kasu, and T. Makimoto, *Appl. Phys. Lett.* **89**, 182112 (2006).
- ¹¹H. Heinke, V. Kirchner, S. Einfeldt, and D. Hommel, *Appl. Phys. Lett.* **77**, 2145 (2000).
- ¹²S. R. Lee, A. M. West, A. A. Allerman, K. E. Waldrip, D. M. Follstaedt, P. P. Provencio, D. D. Koleske, and C. R. Abernathy, *Appl. Phys. Lett.* **86**, 241904 (2005).
- ¹³A. A. Allerman, M. H. Crawford, A. J. Fischer, K. H. A. Bogart, S. R. Lee, D. M. Follstaedt, P. P. Provencio, and D. D. Koleske, *J. Cryst. Growth* **272**, 227 (2004).
- ¹⁴K. X. Chen, Q. Dai, W. Lee, J. K. Kim, E. F. Schubert, W. Liu, S. Wu, X. Li, and J. A. Smart, *Appl. Phys. Lett.* **91**, 121110 (2007).
- ¹⁵M. Albrecht, A. Cremades, J. Krinke, S. Christiansen, O. Ambacher, J. Piqueras, H. P. Strunk, and M. Stutzmann, *Phys. Status Solidi B* **216**, 409 (1999).
- ¹⁶S. J. Henley and D. Cherns, *J. Appl. Phys.* **93**, 3934 (2003).
- ¹⁷J. C. Zhang, D. S. Jiang, Q. Sun, J. F. Wang, Y. T. Yang, J. P. Liu, J. Chen, R. Q. Jin, J. J. Zhu, H. Yang, T. Dai, and Q. J. Jia, *Appl. Phys. Lett.* **87**, 071908 (2005).
- ¹⁸I.-H. Lee, I.-H. Choi, C.-R. Lee, and S. K. Noh, *Appl. Phys. Lett.* **71**, 1359 (1997).
- ¹⁹K. X. Chen, Y. A. Xi, F. W. Mont, J. K. Kim, E. F. Schubert, W. Liu, X. Li, and J. A. Smart, *J. Appl. Phys.* **101**, 113102 (2007).